Sensors and Materials, Vol. 18, No. 7 (2006) 367–380
MYU Tokyo

S & M 0656

Development and Characterization of 4,4-Dithiodibutyric Acid as a Monolayer for Protein Chips

Ling-Sheng Jang* and Hao-Kai Keng[1]

Department of Electrical Engineering and Center for Micro/Nano Science and Technology,
National Cheng Kung University, Taiwan
[1]Institute of Nanotechnology and Microsystem Engineering,
National Cheng Kung University, Taiwan

(Received July 7, 2006; accepted September 26, 2006)

Key words: self-assembled monolayer, 4,4-DTBA, 11-MUA, protein chip

Despite considerable effort, the fabrication of protein chips using a self-assembled monolayer (SAM) with a long chain remains a challenge, due to its steric hindrance and the formation of disulfides, which may generate multilayers and block the terminal carboxylate groups of the SAMs, and thus reduce the sensitivity of the chips. To eliminate those problems, the feasibility of using a short-chain SAM, 4,4-dithiodibutyric acid (4,4-DTBA, disulfide), as a monolayer for the protein chips based on a gold surface was studied. Experiments for characterizing 4,4-DTBA were performed by contact angle goniometry, atomic force microscopy (AFM), Fourier transform infrared spectroscopy (FTIR) and ellipsometry. Additionally, a fluorescent assay of 4,4-DTBA was performed using protein A-fluorescein isothiocyanate (FITC). The results of 4,4-DTBA were compared with those of 11-mercapto-undecanoic acid (MUA). The comparison results indicate that 4,4-DTBA can be adopted as a monolayer for protein chips.

1. Introduction

Protein chips have recently been extensively studied because chips such as protein-based biosensors play an important role in immunoassay for clinical medicine and disease diagnosis. Protein-based biosensors are composed of an immobilized protein layer and a physical transducer,[(1–3)] and can be fabricated using small amounts of proteins and reagents by immobilizing several hundreds or thousands of different proteins on the substrates. However, controlling the configuration of the immobilized antibodies without decreasing the sensitivity of protein immunoassay has become important. The surface area available for a binding antibody affects assay sensitivity and reproducibility. Antibodies in conven-

*Corresponding author, e-mail address: lsjang@ee.ncku.edu.tw

tional immunoassays are generally bound on surfaces of at least 100 mm^2.[4] Thus, one of the important factors in immunosensor design is the choice of the immobilization method, in terms of retaining the activity of the protein. Several methods, including physical adsorption and chemical covalent binding, have been presented for preparing oriented protein and antibody molecular layers on solid matrix substrates.[5–8] To enhance the sensitivity of the sensor, the distance between the transducer surface and the immobilized layer of antibodies should be minimized, and the monolayer on the surface should be two-dimensional in character.[9]

Self-assembled monolayer (SAM) technology has recently been studied for its application to fabricating protein and antibody molecular layers on solid surfaces. Many fundamental and central biological recognition systems require biological surfaces to be biocompatible interfaces for transduction.[10,11] A protein biosensor requires an artificial biomolecular monolayer. SAMs have recently become of interest in bio-micro-electro-mechanical system (MEMS) technology due to their versatility for bio-applications. SAMs are a powerful tool for generating monolayers for fabricating protein biosensors. With the demand for SAMs owing to their functionality, studies of the surface modification using SAMs are another interesting approach to MEMS technology. SAMs can be used in a robust method for fabricating protein monolayers.[12] Pure SAMs of thiol and disulfide with different chain lengths and terminal groups on a gold surface have been studied for several years.[13,14] These studies revealed the formation of a well-ordered monolayer of n-alkanethiols ($CH_3(CH_2)_xSH$, $x > 10$) on gold. The long-chain thiol generally has a long alkyl chain and van der Waals attractive forces among the molecules, which result in high packing density and well-ordered structures of SAMs.[15–17] However, the SAMs of pure long-chain thiol have several problems, such as high densities of surface terminal groups leading to steric hindrance[18,19] and the formation of multilayer caused by deposition of disulfides resulting from the oxidation of thiols.[20] Additionally, the length of the aliphatic chain markedly affects the rates and extents of oxidation and desorption.[21] Moreover, the thiols of long-chain SAMs are unstable in EtOH solution.[22] Therefore, short-chain SAMs have drawn attention as a monolayer in the biochip technology.[23,24]

The activity of proteins such as immunoglobulin (IgG) immobilized on a solid surface is typically lower than that in the aqueous phase. The main reason for the activity reduction is the random orientation of the protein molecules on the solid substrate. A well-known protein A is adopted as a binding material to improve and construct a well-defined antibody surface. Protein A, a cell wall component of *Staphylococcus aureus*, can bind to the Fc part of the antibody. Therefore, the use of protein A leads to highly efficient immunoreactions, and enhances detection system performance.[25–30]

Proteins require much care to maintain its three-dimensional structure and bioactivity function owing to their unique properties, particularly their sensitivity to substrate surfaces. The fabrication of nanoscale structures with SAMs to combine protein A with solid substrates has attracted much attention owing to the interest in a two-dimensional molecular assembly and its potential applications in molecular devices, sensors and surface engineering.

In this study, a short-chain SAM, 4,4-DTBA, was investigated as an alternative monolayer for the protein chip based on a gold surface. The results of 4,4-DTBA were

compared with those of the long-chain SAM, 11-mercapto-undecanoic acid (MUA), which was mostly used. The monolayers fabricated using 4,4-DTBA and 11-MUA were characterized by contact angle, Fourier Transform Infrared Spectroscopy (FTIR), Atomic Force Microscope (AFM), and ellipsometry. Additionally, protein A-FITC was immobilized on self-assembled monolayers with 1-(3-dimethylamino-propyl)-3-ethylcarbodiimide hydrochloride (EDC)/ *N*-hydroxycuccinimide (NHS) to demonstrate the feasibility of 4,4-DTBA as a monolayer for the protein chip.[31]

2. Methods and Materials

The experiments were divided into two sections, that using a 4,4-DTBA SAM and that using a 11-MUA SAM. For each SAM, the concentrations of the solution were 10, 20, 40, 80 and 160 mM. The concentration of protein A-FITC was 0.0167 mg/ml. Surface-grafted polymers such as OEG are well known for preventing protein adsorption, and are widely used for surface modification because of their unique properties such as hydrophilicity, flexibility, high exclusion volume in water, nontoxicity and nonimmunogenecity.[32–36] To improve the nonspecific binding, (*N*-triethoxysilylpropyl)*o*-polyethylene-oxide urethane (PEOU, 3L-4197, Gelest, Inc., United Kingdom) with a terminal OEG functional group was dissolved in THF to prevent the adsorption of protein A-FITC on the substrates.

2.1 *Preparation of gold substratses*

Silicon (75 × 25 mm, Woodruff Tech., USA) was used as the solid support. The substrates were cleaned using piranha (H_2SO_4:H_2O_2=1:3) and sequentially rinsed using distilled water, acetone, isopropanol and distilled water. A photoresist was then patterned on the substrates by photolithography. Titanium (Ti) with a thickness of 150 nm was initially sputtered onto the silicon substrate as an adhesion layer, followed by a 650 nm layer of gold (Au) sputtered using an E-beam evaporator. The substrate was cleaned using acetone to peel off the gold by the lift-off technique, and immersed in ethanol solution for 30 min. Finally, the gold patterns were fabricated on the silicon substrate. Figure 1 shows the fabricated gold substrate.

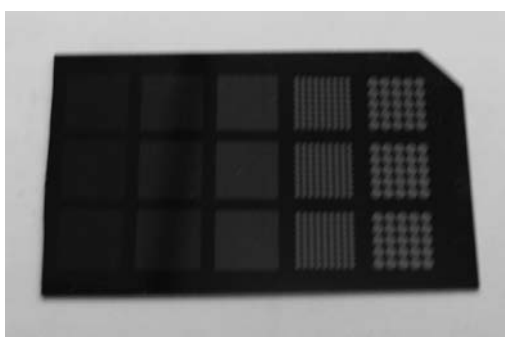

Fig. 1. The fabricated gold substrate.

2.2 *Formation of monolayers*

The gold substrates were cleaned using a hot solution of HCl / H_2O_2 / distilled water (1:1:6, v/v) for 15 min, and rinsed with distilled water. The clean substrates were immersed into silaned OEG / tetrahydrofuran (THF) (1:10, v/v) solution for 12 h.[34] The substrates were then immersed in 11-MUA (450561-5G, Sigma-Aldrich) and 4,4-DTBA (C15605-10G, Sigma-Aldrich) ethanolic solution with concentrations of 10, 20, 40, 80 and 160 mM for 24 h. The residual self-assembled monolayers were then washed with degassed ethanol three times using an ultrasonic cleaner, and dried in a stream of nitrogen.

2.3 *Immobilization of protein A-FITC*

Additionally, the treated samples were immersed in EDC (03450, Fluka, USA) / NHS (56480, Fluka, USA), 75 mM/25 mM, which had been dissolved in PBS buffer (pH 7.4; 0.2 g KCl, 1.44 g $NaHPO_4$, 8 g NaCl and 0.24 g KH_2PO_4 in 1 L of distilled water) for 4 h, and again dried in a stream of nitrogen. A drop of protein, A-FITC, with a concentration of 0.0167 mg/ml (P3838, Sigma, USA) was placed on the treated substrates. The samples were then incubated at 4°C for 24 h to immobilize protein A-FITC onto the substrates. Figure 2 shows a schematic of the two-step reaction scheme employed to immobilize protein A on a self-assembled monolayer.

2.4 *Measurement of contact angle*

The contact angles of droplets on the substrate were measured by contact angle goniometry (MigicDrop, Future Digital Scientific Corp., USA). The relative humidity in the environment was 47%, and the temperature varied between 25 and 27°C. The volume of the droplet was 5 μl. The gold substrates were initially immersed in the solutions of SAMs with a concentration of 10 mM for 2, 4, 6, 8 and 24 h, and then immersed into solutions of 10, 20, 40, 80 and 160 mM SAMs for 24 h. The substrates were then cleaned with ethanol and dried in a N_2 stream. Finally, the contact angles of the modified surface with the 4,4-DTBA and 11-MUA SAMs were measured to determine whether the SAMs had successfully been fabricated onto the gold substrates. All the reported values are averages of at least six measurements taken at different locations on the film surface.

2.5 *FTIR*

The gold substrates (15 × 15 mm) were treated with solutions of SAMs. The treated substrates were analyzed using FTIR (DA-8.3, Bomem, Canada). The FTIR spectra were obtained by reflecting a ρ-polarized beam from the gold surface at the near-glancing angle of incidence of 75°. The instrumentation comprised a modified Digilab 15B Fourier transform spectrometer system equipped with a liquid-nitrogen-cooled MCT narrow band detector, and was operated at a resolution of 2 cm^{-1}. The SAMs were studied in accordance with the wave number peak of the alkyl chain groups (CH_2 groups).

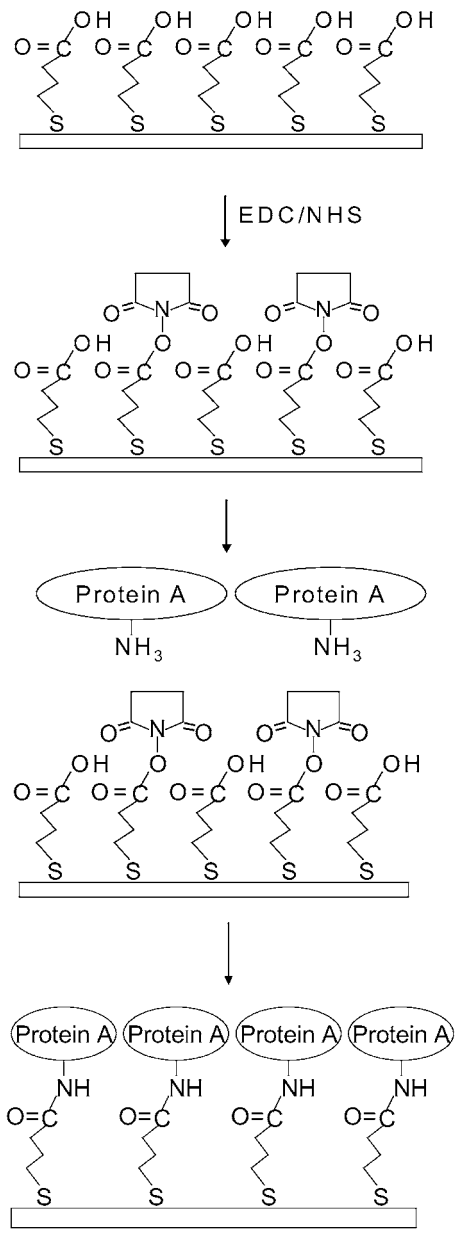

Fig. 2. Two-step reaction scheme employed to immobilize protein A on self-assembled monolayer.

2.6 *AFM*

The surface topologies of the 4,4-DTBA and 11-MUA SAMs were examined by AFM (P7L, NT-MDT, USA). The samples (15 × 15 mm) were measured by AFM operated in the tapping mode in air and at room temperature. Images were acquired at a scan rate of 1.5 Hz using a silicon cantilever, and the scan size was 2 × 2 μm. The surface roughness (Ra) for each AFM image was determined using the software provided with the instrument.

2.7 *Ellipsometry*

The samples (15 × 15 mm) were treated with the SAM solutions. Ellipsometric measurements were performed at room temperature using a modified traditional null-type ellipsometer equipped with a polarizer-compensator-sample-analyzer (PCSA) arrangement and a He-Ne laser light source (632.8 nm) as the light source.[37,38] The ellipsometer was operated at wavelengths of 400–800 nm at an angle of 75°. The ellipsometric data were obtained with an average of five points for each sample using a 3-phase model. Figure 3 shows a schematic of the ellipsometric 3-phase model.

2.8 *Characterization of binding capacity using protein A-FITC*

Fluorescence images were characterized for studying the immobilization of protein A-FITC with SAMs based on the ratio of fluorescent area to total area against fluorescence intensity. The results were then normalized in accordance with the fluorescence intensity of the control sample. The fluorescence images were taken using a CCD camera (Evoluting VF, Q-imaging, USA) and analyzed using Image-Pro Plus 5.0 (Media Cybernetics, USA).

3. Results and Discussion

3.1 *Contact angle analysis*

The activation of 4,4-DTBA and 11-MUA utilizing contact angle goniometry was observed in this study. Figures 4 and 5 show the results of this analysis. The contact angle of the uncleaned surface was 82.4° ± 2.1°. After washing with a hot solution of HCl / H_2O_2 / distilled water (1:1:6, v/v), the contact angle was reduced to 71.8° ± 2.3°. The surfaces of the substrates became more hydrophilic after treating the hot solution. Figure 4 shows the contact angles obtained for 4,4-DTBA and 11-MUA at a concentration of 10 mM for different immersion times. According to Fig. 4, the gold surfaces modified by the SAM solutions became increasingly hydrophilic as the contact angle decreased and the SAM immersion time increased. The contact angle of the 11-MUA layer decreased to 58.1° ± 1.14° after 2 h, but that of the 4,4-DTBA decreased slightly to 71.3° ± 0.43°. With

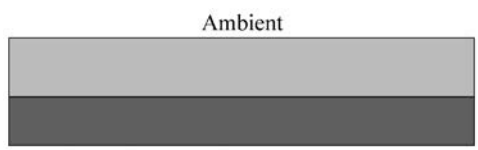

Fig. 3. Schematic of ellipsometric three-phase model.

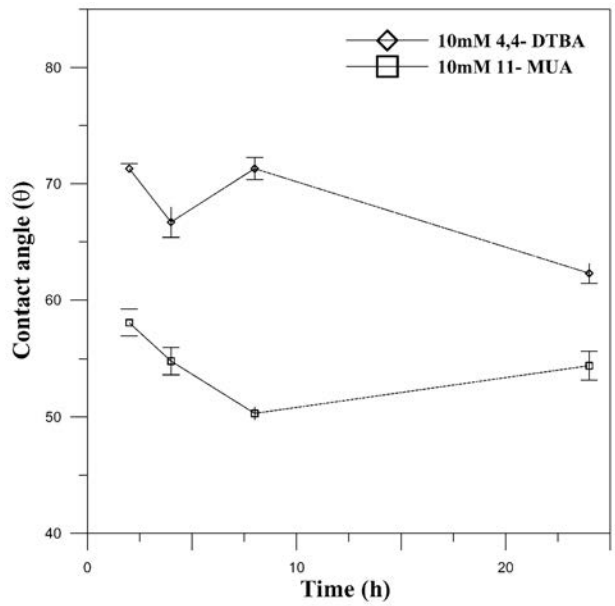

Fig. 4. Contact angle vs immersion time plots for 10 mM 4,4-DTBA and 10 mM 11-MUA.

increasing immersion time, the 11-MUA contact angle decreased from 58.1° to 50.3°. After 24 h, the contact angle of 11-MUA was 54.4° ±1.24°, and that of 4,4-DTBA was 62.3° ±0.87°. Figure 5 shows the contact angles of 4,4-DTBA and 11-MUA. The angles were 52.5° ±0.78° after the substrate was immersed in 10 mM 11-MUA for 24 h, and 57.3° ± 0.65° for 4,4-DTBA. However, the contact angles of both 4,4-DTBA and 11-MUA decreased as the concentration increased indicating that the gold surface became increasingly hydrophilic. Finally, the contact angle of a 160 mM solution of 4,4-DTBA was 42.5° ± 0.87°, and that of 11-MUA was 31.9° ± 0.61° after 24 h. The experimental results indicate that the self-assembled monolayer was successfully fabricated onto the gold substrates. In order to ensure the successful immobilization of SAMs on the substrate, the samples were immersed in SAM solutions for 24 h in the following characterizations.

3.2 *Characterization of self-assembled monolayer by FTIR*

The SAMs were analyzed by FTIR to ensure that they were well ordered and had bonded successfully. Figure 6 shows the FTIR data for 160 mM 4,4-DTBA and 160 mM 11-MUA. The SAMs on the solid substrate were characterized using reflection IR spectroscopy. This investigation adopted the assumption that the strongest adsorption occurs for vibrational modes with transition dipoles oriented perpendicular to the gold surface, whereas virtually no adsorption occurs for dipoles parallel to the surface. The CH_2 groups of all sulfides and disulfides herein exhibited C-H stretching frequencies with 2916 – 2926 cm^{-1} higher than those of pure crystalline compounds. A wave number of a CH_2 peak

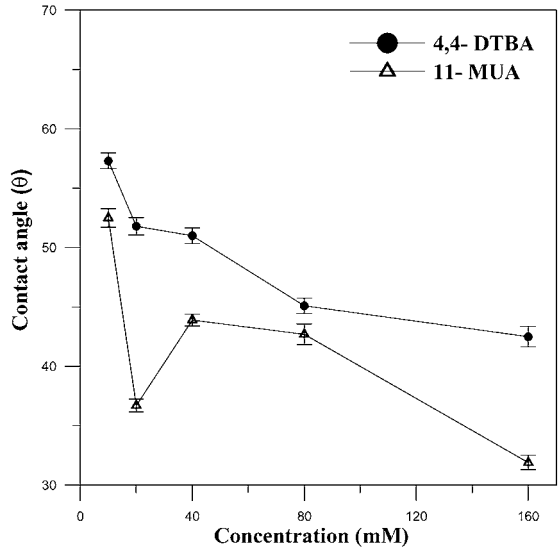

Fig. 5. Contact angle vs concentration plots for 4,4-DTBA and 11-MUA.

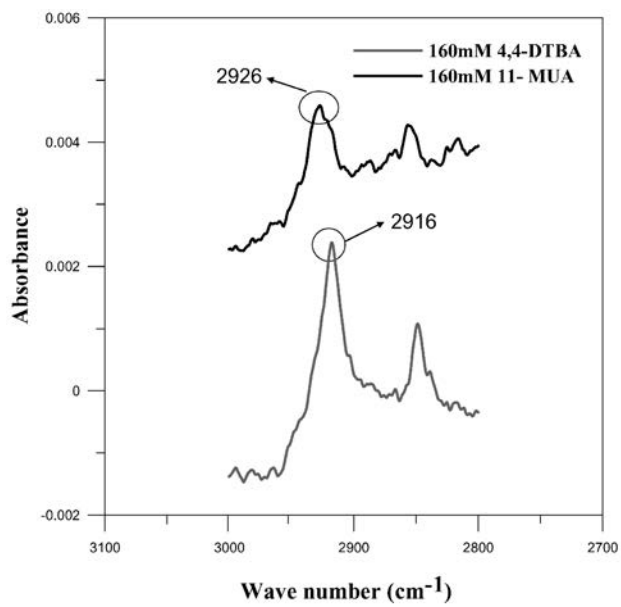

Fig. 6. FTIR spectra of 160 mM 4,4-DTBA and 160 mM 11-MUA.

close to 2926 cm^{-1} means that the structure of the SAM is highly disordered. A wave number close to 2918 cm^{-1} signifies that the structure of the SAM is well ordered on the solid substrate. Finally, a wave number close to 2916–2917 cm^{-1} means an exceptionally high quality order. From Fig. 6, the infrared spectrum clearly exhibits peaks of 160 mM 4,4-DTBA and 160 mM 11-MUA at 2916 and 2926 cm^{-1}, respectively. The experimental results reveal that the self-assembled monolayer of 4,4-DTBA are successfully arranged and ordered.

3.3 *Topography analysis using AFM*

The surface roughness of the gold substrates immobilized by 4,4-DTBA and 11-MUA was characterized by AFM. The surface roughness is generally obtained from the interaction force between the sample and the probe. A well-organized molecular array can then be observed on the nanoscale. The surface roughnesses of the 11-MUA layer and 4,4-DTBA layer on the gold substrate are shown in Fig. 7 measured using this approach. The surface roughnesses of 4,4-DTBA were 0.7 nm at a concentration of 10 mM and 0.5 nm at 160 mM. The surface roughnesses of 11-MUA was 0.9 nm at 10 mM, and 4.1 nm at 160 mM. The increasingly surface roughness of 11-MUA may be caused by disulfides that were oxidized from thiols. Disulfides could precipitate onto the SAMs/Au surface as a result of the interaction between the terminal methyl groups of the SAMs/Au.[20] The above results demonstrate that 4,4-DTBA can be a uniform layer for protein chips.

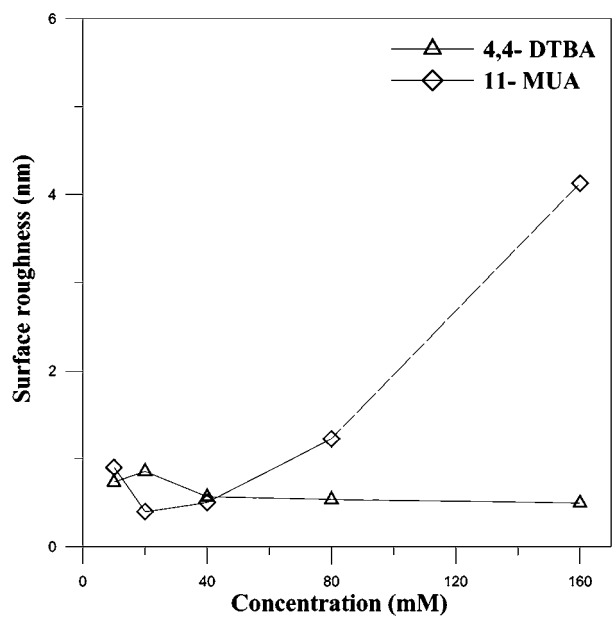

Fig. 7. Surface roughness vs concentration plots for 4,4-DTBA and 11-MUA.

3.4 *Thickness measurement using ellipsometry*

The thicknesses of the 4,4-DTBA and 11-MUA layers were computed by ellipsometry. Ellipsometry is an important tool for investigating various aspects of the structures of thin films, such as their thickness, optical parameters and deposition kinetics. An ellipsometer was used to measure the change in the state of polarization for reflected polarized light. In this study, the thickness of SAMs was measured using the complex refractive index, $N = n + k_i$, $N = 1.45$. For ellipsometry, the underlying Si wafer was assumed not to affect the spectra of ellipsometric angle, because the gold was deposited thickly onto the Si wafer (150 nm). In this study, the optical model consisted of gold, interface (SAM) and ambient layer (air). This three-phase layer model adopted an interface to model the roughness of the gold surface using the Bruggeman effective-medium approximation (EMA). When the fitting procedure was completed with the void volume fraction and thickness of the interface layer as unknown variables, the optical model was optimized at 38% for the void volume fraction, and the thicknesses of the 11-MUA and 4,4-DTBA layers were found to be 1.61 ± 0.17 nm and 0.54 ± 0.01 nm, respectively, as shown in Fig. 8. Figure 8 shows that the thickness of 4,4-DTBA was more stable than that of 11-MUA, and did not increase with concentration. Since the disulfide of 4,4-DTBA is more stable than thiol in EtOH solution, it may reduce the deposition of disulfides onto the substrate, which is formed by the oxidization of thiols.[20–22] According to the results, 4,4-DTBA can be a suitable monolayer, and its functionality is unaffected by concentration.

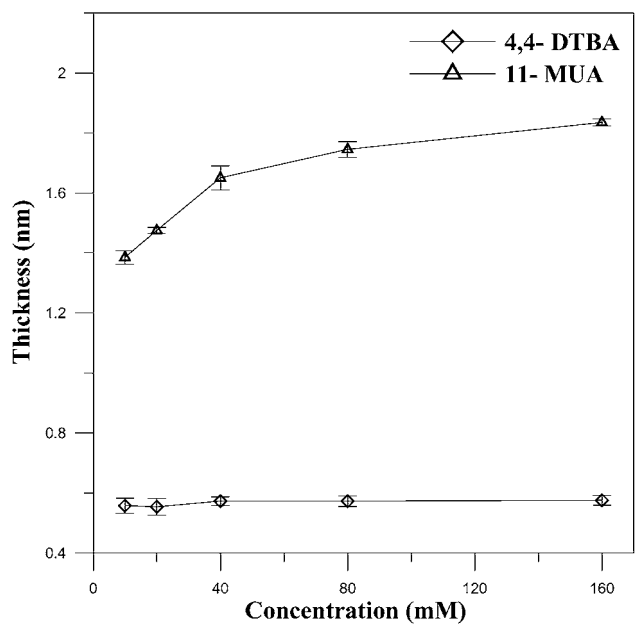

Fig. 8. Thickness vs concentration plots for 4,4-DTBA and 11-MUA.

3.5 *Characterization of immobilization with protein A-FITC*

Finally, the SAMs at concentrations of 160 mM were used to immobilize the protein A-FITC on the SAM. Figures 9(a) and 9(b) show fluorescence images of the protein A-FITC on the 4,4-DTBA and 11-MUA layers, respectively. The graphs in Fig. 10 demonstrate that 4,4-DTBA had a higher ratio of fluorescent area to total area, and a higher fluorescence intensity than 11-MUA. The distribution of the fluorescence intensity of 11-MUA in Fig. 10 was in the range of 0.3–0.8, with a high ratio of fluorescent area to total area, whereas that of 4,4-DTBA was in the range 0.53–0.98, and also with a high ratio of fluorescent area to total area. The fluorescence intensity of 4,4-DTBA was higher than that of 11-MUA. The experimental results demonstrate that the protein A-FITC was successfully immobilized onto 4,4-DTBA.

4. Conclusions

The contact angles obtained from the characterizations of 4,4-DTBA and 11-MUA on the gold surfaces indicate that 4,4-DTBA and 11-MUA SAMs were successfully fabricated on the gold substrates. According to the FTIR data, the wave number peaks of 4,4-DTBA and 11-MUA were 2916 and 2926 cm^{-1}, respectively. The FTIR results show that 160 mM 4,4-DTBA was successfully arranged and ordered. Additionally, the topography and ellipsometry of 4,4-DTBA were analyzed to demonstrate that 4,4-DTBA was a monolayer. The surface roughnesses of the 4,4-DTBA and 11-MUA layers at 160 mM were 4.1 and 0.5 nm, respectively. Finally, the fluorescence images indicate that the protein A-FITC was successfully immobilized on 4,4-DTBA. We conclude from the experimental results that a 4,4-DTBA SAM can be used as a monolayer for protein chips.

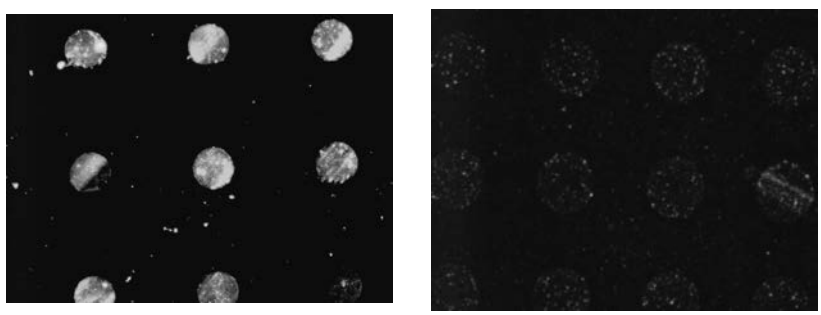

(a) (b)

Fig. 9. Fluorescence images of (a) 160 mM 4,4-DTBA and (b) 160 mM 11-MUA.

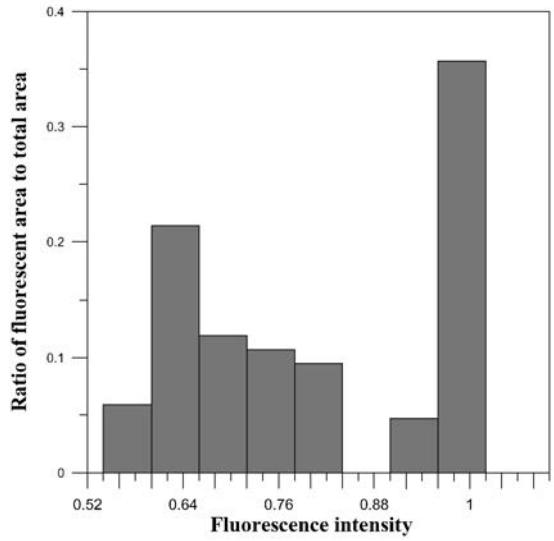

(a)

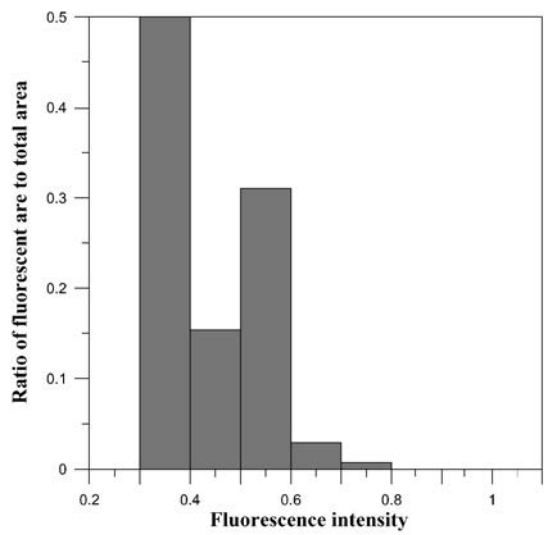

(b)

Fig. 10. Distributions of fluorescence intensity with protein A-FITC on (a) 160 mM 4,4-DTBA and (b) 160 mM 11-MUA.

Acknowledgements

The authors would like to thank the National Science Council of Taiwan for financially supporting this research under Contract No. NSC 94-2622-E-006-044-CC3 and NSC 94-2218-E-006-043. The authors would also like to thank the Center for Micro/Nano Science and Technology, National Cheng Kung University, Tainan, Taiwan, for access to equipment and technical support. Furthermore, this work made use of Shared Facilities supported by the Program of Top 100 Universities Advancement, Ministry of Education, Taiwan.

References

1 E. Shin, K. Lee and Y. Lee : Journal of Microbiology and Biotechnology **10** (2000) 595.
2 G. G. Guilbault, B. Hock and R. Schmid: Biosens. Bioelectron. **7** (1992**)** 411.
3 C. S. Liao, G. B. Lee, J. J. Wu, C. C. Chang, T. M. Hsieh, F. C. Huang and C. H. Luo: Biosens. Bioelectron. **20** (2005) 1341.
4 R. P. Ekins: Clin. Chem. **44** (1998) 2015.
5 S. Kanno, Y. Yanagida, T. Haruyama, E. Kobatake and M. Aizawa: J. Biotechnol. **9** (2000) 376.
6 Y. S. Lo, N. D. Huenfner, W. S. Chen, F. Stecens, J. M. Harris and T. P. Beebe: Langmuir **15** (1999) 1373.
7 R. J. Pei, J. M. Hu, Y. Hu and Y. Zeng: J. Chem. Technol. Biotechnol. **73** (1998) 59.
8 G. B. Sigal, C. Bamddad, A. Barberis, J. Strominger and G. M. Whitesides: Anal. Chem. **68** (1996) 490.
9 T. Dubrovsky, A. Tronin, S. Dubrovskaya, S. Vakula and C. Nicolini: Sens. Actuators, B **23** (1995) 1.
10 T. L. Breen, J. Tien, S. R. J. Oliver, T. Hadzic and G. M. Whitesides: Science **284** (1999) 948.
11 H. G. Choi, B. K. Oh, W. H. Lee and J. W. Choi: Biotechnol. Bioprocess Eng. **6** (2001) 183.
12 W. G. Koh and M. Pishko: Sens. Actuators, B **106** (2005) 335.
13 O. Emanuele, Y. Lin and M.W. George: Colloids Surf., B **15** (1993) 3.
14 G. Henrik, A. Curioni and W. Andreoni: J. Am. Soc. **122** (2000) 2829.
15 Y. M. Bae, B. K. Oh, W. Lee, W. H. Lee and J. W. Choi: Biosens. Bioelectron. **21** (2005) 103.
16 S. J. Hinder, S. D. Connell, M. C. Davies, C. J. Roberts, S. J. B. Tendler and P. M. Wiliams: Langmuir **12** (2002) 3151.
17 J. Noh, H. S. Kato, M. Kawai and J. M. Hara: Phys. Chem. **106 (**2002**)** 13268.
18 J. W. Lee, S. J. Sim and S. M. Cho: Biosens. Bioelectron. **20** (2005) 1422.
19 Y. T. Kim, R. L. McCarley and A. J. Bard: Langmuir **9** (1993) 1941.
20 W. Lee, D. Bong, B. K. Oh, W. H. Lee and J. W. Choi: Enzyme Microb. Technol. **35 (**2004**)** 678.
21 M. C. Wang, J. D. Liao, C. C. Weng, R. Klauser, A. Shaporenko, M. Grunze and M. Zharnikov: Langmuir **19** (2003) 9774.
22 N. Prathima, M. Harini, N. Rai, R. H. Chandrashekara, K. G. Ayappa, S. Sampath and S. K. Biswas: Langmuir **21** (2005) 2364.
23 T. Hasunuma, S. Kuwabata, E. Fukusaki and A. Kobayashi: Anal. Chem. **76** (2004) 1500.
24 M. R. Malone, J. F. Masson, S. Beaudoin and K. S. Bookh: Proc. of SPIE **6007** (2005) 60070A-1.
25 H. Neubert, E. S. Jacoby, S. S. Bansal, R. K. lles, D. A. Cowan and A. T. Kicman: Anal. Chem. **74** (2002**)** 3677.

26 S. F. Chou, W. L. Hsu, J. M. Hwang and C. Y. Chen: Biosens. Bioelectron. **19** (2004) 999.
27 S. Susmel, C. K. O'Sullivan and G. G. Guilbault: Enzyme Microb. Technol. **27** (2000) 639.
28 M. Akram, M. C. Stuart and D. K.Y. Wong: Anal. Chim. Acta. **504** (2004) 243.
29 T. Tanaka and T. Mastsunaga: Anal. Chem. **72** (2000) 3518.
30 I. C. Goncalves, M. Cristina L. Martins, M. A. Barbosa and B. D. Ratner: Biomaterials **26** (2005) 3891.
31 B. K. Oh, W. Lee, B. S. Chun, Y. M. Bae, W. H. Lee and J. W. Choi: Colloids Surf., A **257** (2005) 369.
32 B. K. Oh, Y. K. Kim, K. W. Park, W. H. Lee and J. W. Choi: Biosens. Bioelectron. **19** (2004) 1497.
33 W. Lee, B. K. Oh, Y. M. Bae, P. S. Hwan, W. H. Lee and J. W. Choi: Biosens. Bioelectron. **19** (2003) 185.
34 S. Y. Oh, H. S. Choi, H. S. Jie and J. K. Park: Mater. Sci. Eng., C **24** (2004) 91.
35 H. Gronbeck, A. Curioni and W. Andreoni: J. Am. Chem. Soc. **122** (2000) 3839.
36 S. W. Lee and P. E. Laibinis: Biomaterials (1998) 1669.
37 Y. M. Bae, B. K. Oh, W. Lee, W. H. Lee and J. W. Choi: Anal. Chem. **76** (2004) 1799.
38 J. Martensson and H. Arwin: Langmuir **11** (1995) 963.